Hindawi Publishing Corporation
Advances in Mechanical Engineering
Volume 2010, Article ID 807610, 10 pages
doi:10.1155/2010/807610

Research Article

Effects of Particle Surface Charge, Species, Concentration, and Dispersion Method on the Thermal Conductivity of Nanofluids

Raghu Gowda,[1] Hongwei Sun,[1] Pengtao Wang,[1] Majid Charmchi,[1] Fan Gao,[2] Zhiyong Gu,[2] and Bridgette Budhlall[3]

[1] *Department of Mechanical Engineering, University of Massachusetts Lowell, Lowell, MA 01854, USA*
[2] *Department of Chemical Engineering, University of Massachusetts Lowell, Lowell, MA 01854, USA*
[3] *Department of Plastic Engineering, University of Massachusetts Lowell, Lowell, MA 01854, USA*

Correspondence should be addressed to Hongwei Sun, hongwei_sun@uml.edu

Received 1 July 2009; Revised 18 September 2009; Accepted 14 October 2009

Academic Editor: Oronzio Manca

The purpose of this experimental study is to evaluate the effects of particle species, surface charge, concentration, preparation technique, and base fluid on thermal transport capability of nanoparticle suspensions (nanofluids). The surface charge was varied by changing the pH value of the fluids. The alumina (Al_2O_3) and copper oxide (CuO) nanoparticles were dispersed in deionized (DI) water and ethylene glycol (EG), respectively. The nanofluids were prepared using both bath-type and probe sonicator under different power inputs. The experimental results were compared with the available experimental data as well as the predicted values obtained from Maxwell effective medium theory. It was found that ethylene glycol is more suitable for nanofluids applications than DI water in terms of thermal conductivity improvement and stability of nanofluids. Surface charge can effectively improve the dispersion of nanoparticles by reducing the (aggregated) particle size in base fluids. A nanofluid with high surface charge (low pH) has a higher thermal conductivity for a similar particle concentration. The sonication also has a significant impact on thermal conductivity enhancement. All these results suggest that the key to the improvement of thermal conductivity of nanofluids is a uniform and stable dispersion of nanoscale particles in a fluid.

1. Introduction

Due to the low thermal conductivities of most common liquids used in heat exchangers, such as water and ethylene glycol, it has become urgent to look into other advanced alternatives. A new type of fluids called nanofluids (suspensions of nanometer-sized particles in various fluids) has been extensively investigated to enhance the heat carrying capacity of fluids although the mechanism behind exceptionally enhanced thermal conductivity of nanofluids is still not well understood. Different mechanisms have been put forth to explain thermal transport enhancement such as interfacial resistance, nanoparticle motion, liquid layering at particle-liquid interface, and nanoparticle clustering [1]. Among them, nanoparticle motion (Brownian motion) [2–9] and nanoparticle clustering [10–15] have attracted most attention. The initial experiments show preferred thermal properties of nanofluids [16–20], such as an order of magnitude higher thermal conductivity than that predicted by conventional theory on heterogeneous two-component mixture. A very small concentration of copper nanoparticle (less than 0.3% volume fraction of 10 nm nanoparticles) can enhance the thermal conductivity of base fluid (ethylene glycol) by up to 40% [21]. On the other hand, the Hamilton and Crosser (HC) model predicts a less than 1.5% improvement in thermal conductivity [22]. In another study [16] where metallic multiwalled carbon nanotubes (MWCNTs) were dispersed in synthetic oil (α-olefin), an astonishing improvement of 160% in thermal conductivity was observed with only a 1.0% volume fraction of MWNT. The authors argue that the three-dimensional network formed by CNTs is responsible for significant thermal conductivity improvement. A recent study shows that the enhancement of thermal conductivity of nanofluids heavily depends on fluid temperature [9, 23] and particle sizes [24, 25]. Herein a two- to fourfold increase in thermal conductivity was observed when

the fluid temperature increased from 21°C to 51°C [23]. However, the hypothesis of thermal transport enhancement due to Brownian motion is being challenged [26–28]. The recent experimental and theoretical investigation strongly suggests that the nanoparticle aggregation (clusters) plays a significant role in the thermal transport in nanofluids. A light scattering method shows that the cluster size (due to aggregation) in a Fe-ethylene glycol nanofluids increases from 1 micron to 2.4 microns during a 50-minute waiting time after sonication [11]. The thermal conductivity can be enhanced due to percolation effect in the aggregates/clusters, especially for highly conducting particles. But sedimentation will increasingly take place when the size of aggregates exceeds a threshold value. The small particle size and short distance between particles increase the probability of aggregation. On the other hand, a low pH value actually means a high surface potential, and in turns a high repulsive energy and less aggregation [14, 29].

This research is focused on a systematic investigation of key parameters that affect the thermal conductivity of nanofluids. These parameters include surface charge, nanoparticle composition and concentration, base fluids, and preparation techniques. The paper starts with nanofluid preparation and the measurement system, followed with comparisons of the obtained results with those published in open literature and predicted by theory, and then the effects of key parameters are discussed and summarized in detail in the end of the paper.

2. Nanofluids Preparation and Experimental Apparatus

2.1. Nanofluid Preparation. Preparation of nanofluids through which nanoparticles should be uniformly dispersed in base fluids is the first step for improvement in thermal conductivity, but its importance is often ignored. The nanofluid does not simply refer to a liquid-solid mixture. Some special requirements are necessary, such as uniform, stable, and durable suspension, low or no aggregation of particles, and no chemical reaction. There are three primary methods being used to prepare nanofluids [29]: (i) direct dispersion of powder form nanoparticles in the base fluids; (ii) nanoparticle synthesized by chemical precipitation and then dispersed in base fluids; (iii) direct nanoparticle synthesis in the base fluid by organic reduction. Stability of the dispersion is ensured by controlling the surface charge of the nanoparticles through the control of the pH value of fluids. This is very effective for oxide nanoparticles such as alumina and copper oxide used in this research.

The nanofluids under current investigation can be divided into two groups based on the base fluids including DI water and ethylene glycol (EG). Both alumina (Al_2O_3) powder (nominal particle size provided by the manufacturer: 40–50 nm) and copper oxide (nominal particle size: 23–37 nm) were purchased from Alfa Aesar for this experiment. These nanoparticles were dispersed in DI water and/or EG (99%, source: Alfa Aesar) using three sonication methods. They are (1) sonication of nanofluids with a probe sonicator (Branson Digital Sonifier 450) at 80% magnitude (maximum power: 450 W) for 2 minutes; (2) another probe sonicator (Omni-Ruptor 250) at 80% magnitude (maximum power: 150 W) for 2 minutes, and (3) a bath sonicator (Model: 75D VWR) for 4.5 hours at maximum power setting (maximum power: 75 W). The alumina and copper oxide nanoparticles were imaged under a Philips EM400 transmission electron microscope (TEM) to obtain information about nanoparticle size and shape (Figure 1). As can be seen in Figure 1, the alumina nanoparticles are roughly spherical in shape but copper oxide nanoparticles show some deviations from spherical shapes. The size of alumna nanoparticles spans a wide range (from a few nm to 55 nm) but copper oxide nanoparticles do not have very small size particles.

The smaller sized alumina particles (nominal size: 10 nm) from a different source (NanoAmor Inc.) were also considered. But it was found that the dispersion of these alumina nanoparticles in DI water is very difficult even after adding various surfactants such as sodium dodecyl sulfate (SDS), cetyltrimethyl ammonium bromide (CTAB), Pluronic P105 and applying long time ultra sonication. No thermal conductivity measurement was conducted for these alumina nanoparticle solutions.

Temperature rise is minimized by utilizing multiple short sonications (instead of a long sonication) and the evaporation of base fluids is avoided by sealing the container with caps during sonication. The power and time settings of the ultra sonicators were chosen in such a way that a better dispersion is achieved with minimum increase in nanofluids temperature. For example, the DI water-based nanofluids reach 50°C after two-minute sonication. The nanofluids temperature returns back to room temperature (24°C) after around 1.5 hours waiting period. Before each measurement, both the pH and temperature of nanofluids are obtained by a pH probe (Mettler Toledo S-47). The temperature of nanofluids is maintained at room temperature during the measurement. Hydrochloric acid (HCl) (36%, VWR Scientific) or sodium hydroxide (NaOH) (99.99%, ACROS Organics)) is used to adjust the pH value of the nanofluids. An in-house equipment (Zetasizer Nano, Malvern Instruments Ltd) was used for zeta potential and size measurements of nanoparticles after dispersion.

2.2. Thermal Conductivity Measurement Apparatus. Transient hot wire method (THW) was adapted by many researchers to determine the thermal conductivity of the nanofluid suspensions [21, 30–35]. The THW method is a simple but effective transient method for measuring thermal conductivity of materials. This method determines the thermal conductivity by observing the rate at which the temperature of a very thin wire increases with time after an abrupt electrical pulse. It can eliminate the error from natural convection since the measurement is completed in a very short time (less than one second). Figure 2 presents the temperature rise of the wire during the thermal conductivity measurement for DI water.

In this research, an isonel coated platinum (source: A-M systems) with 25 μm in diameter and 15 cm in length

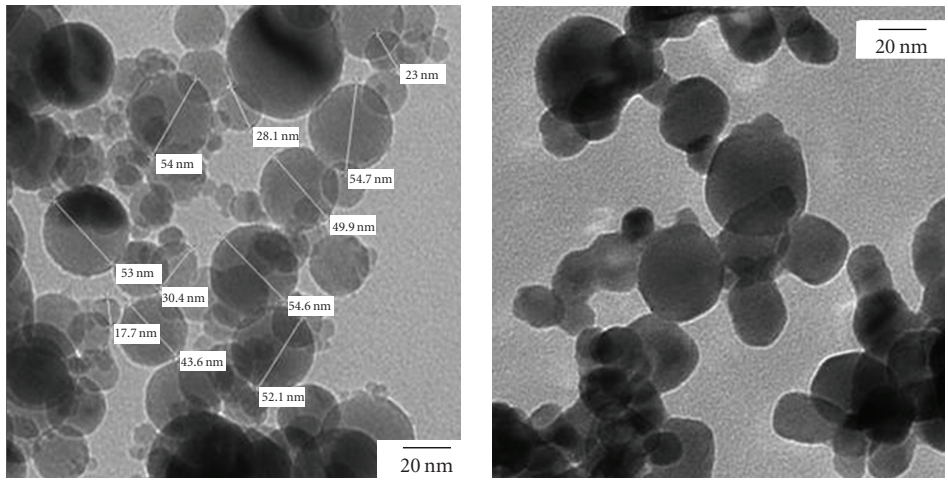

(a) (b)

Figure 1: TEM images of alumina (a) and copper oxide (b) nanoparticles.

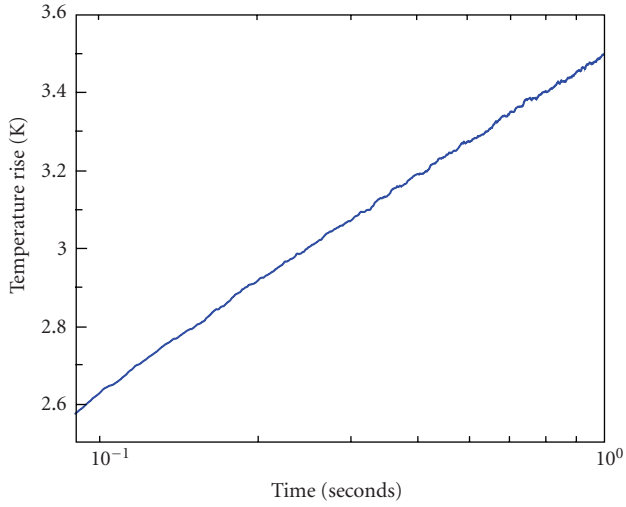

Figure 2: Temperature rise of the hotwire in DI water versus time (with time plotted on log scale).

was immersed horizontally in a plexiglass cell ($17 \times 2 \times 2.5$ cm) containing nanofluid (see Figure 3(b)). During the experiment, the wire serves as a heat source, a thermometer, as well as one of the legs of a Wheatstone bridge (Figure 3(a)). The temperature rise of the wire is calculated from the change in the resistance of the platinum wire with time, obtained by measuring the voltage offset using a data acquisition system (DAQ) (NI SCXI-1303). The R_1, R_2, and R_3 represent temperature compensated precision resistors (40 kΩ) in Figure 3(a). R_W and R_P denote the hot wire and the variable resistor to balance the Wheatstone bridge circuit, respectively. Before connecting platinum wire in the experimental system, the platinum wire was calibrated in a constant temperature bath and the measured temperature coefficient of resistance was 0.0033524 Ω/ΩK. The derivation of Fourier's equation for an infinite line heat source in an infinite heat medium gives us the following equation:

$$k = \frac{q}{4\pi L}\left(\frac{\ln(t)}{\Delta T}\right), \tag{1}$$

where k is the thermal conductivity of the fluid, q is the heat dissipation rate. L is the length of the wire and t the time (from start of heating), and ΔT is the temperature rise of the wire. Therefore, the temperature rise (ΔT) versus natural log of time (t) data were plotted and the slope was then used to calculate the thermal conductivity (Figure 2) and a linear relationship implies that conduction is the primary mode of heat transfer during the measurement [32]. The experiment lasts for around 5 seconds. The slope of the straight line in the curve ($\ln(t)/\Delta T$) between 0.1 and 1 second was used for the calculation of thermal conductivity (Figure 2).

The calibration of the apparatus was performed by comparing the measured thermal conductivities of DI water and EG with those from literature values at room temperature [36]. Deviation for DI water and EG is 0.66% and 2.36%, respectively. The uncertainty analysis of measured thermal conductivity was attached in the appendix. Each thermal conductivity value was obtained from an average of 20 measurements with an estimated accuracy of ± 0.0015 and ± 0.0013, respectively [37]. These results demonstrate that the experimental setup used in the present work can produce a reliable thermal-conductivity data. Additional details of the apparatus and technique are available elsewhere [32].

3. Results and Discussion

3.1. Comparison with Published Literature. The thermal conductivities of alumina/DI water, alumina/EG, and copper oxide/EG are compared with available published results [38–42]. The nanofluids were dispersed using the bath sonicator and the results are presented in Figures 4, 5, and 6. The experimental results are consistent with other published

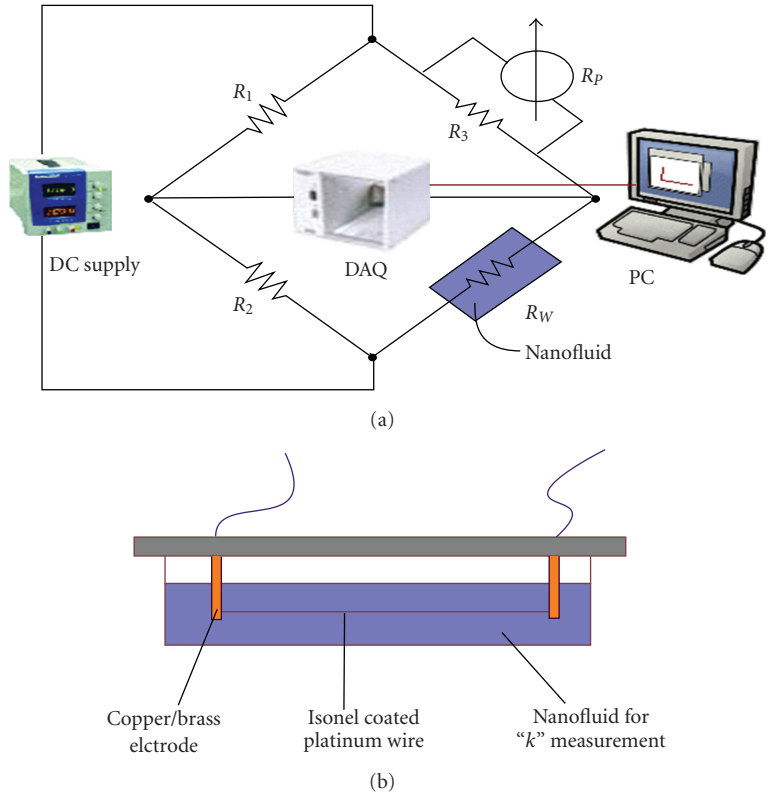

Figure 3: (a) Schematic of transient hot wire (THW) system and (b) test cell containing platinum wire and nanofluids.

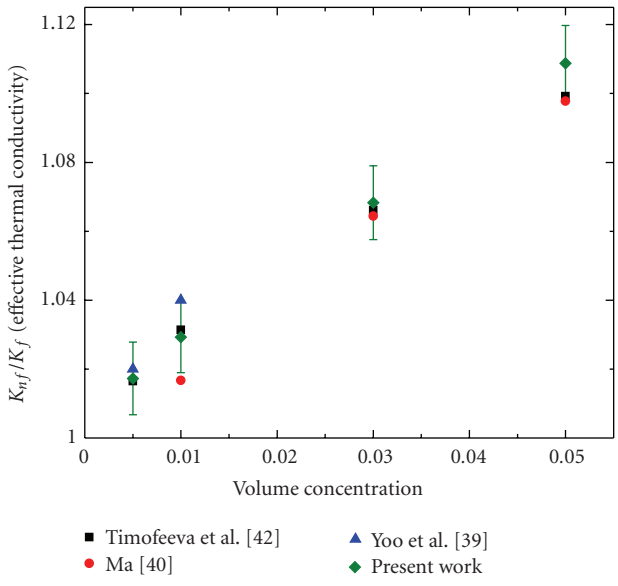

Figure 4: Comparison of experimental data of DI water-based alumina nanofluids with literature data [39, 40, 42].

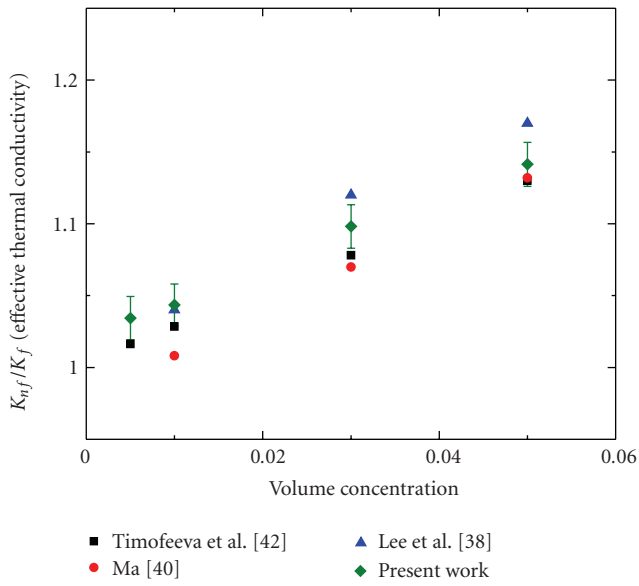

Figure 5: Comparison of experimental data of EG-based alumina nanofluids with literature data [38, 40, 42].

results within the experimental uncertainty. The thermal conductivity increases with the increase of volumetric fraction of nanofluids. Apparent density values for alumina (4.0 g/cm^3) and copper oxide (6.4 g/cm^3) were used for volume fraction calculations.

3.2. Effect of pH Value on Thermal Conductivity. Surface charge is critical for the stabilization of colloidal solutions. The effect of pH value on thermal conductivity of DI water-based alumina nanofluids was examined in this work. The pH values of alumina/DI water were changed from 7.0 to

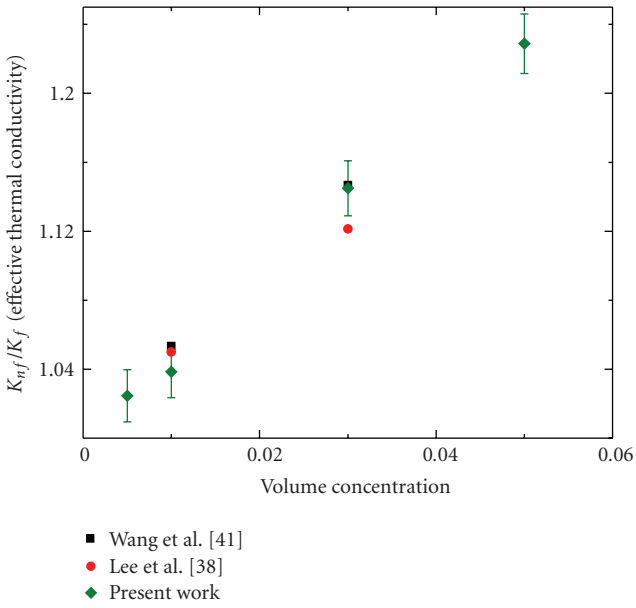

Figure 6: Comparison of experimental data for EG-based copper oxide nanofluids with literature data [38, 41].

2.0 by adding HCl solution into the nanofluids. By adding NaOH solutions, the values of 7.0 to 11.0 were obtained. The nanoparticles were dispersed using bath sonicator with parameters mentioned above. The corresponding thermal conductivities were measured using THW apparatus and plotted in Figure 7(a). As a comparison, the prediction from effective medium theory (EMT) is also plotted (solid line) [42]. The EMT gives a relationship between particle volume fraction and thermal conductivity improvement solely based on particle volume concentration (ϕ) as described below

$$\frac{K_{nf}}{K_F} = 1 + 3\phi. \tag{2}$$

The EMT theory is conventionally employed when (1) the particles are assumed to be static; (2) thermal conductivity of the particles is much higher than that of base fluid; (3) the volume fraction of particles is small; (4) the shape of particles is spherical. Compared with abnormal improvement in thermal conductivity reported by published results, overall the present thermal conductivity results of alumina nanofluids are lower than the values from the prediction from EMT theory. Our finding is consistent with published results by Timofeeva et al. [42]. The conclusion was made that the low thermal conductivity is mainly caused by aggregation of nanoparticles. One consequence of the aggregation is the reduction of particle numbers in solution and size increase (clustered structures) of particles. The impact of these mechanisms on thermal conductivity enhancement is complicated depending on the primary mechanism for heat transport. On one hand, the size increase of particles in nanofluids forms fractal/clustered structures in fluids which will shorten the heat conduction path in medium, so the thermal conductivity should be

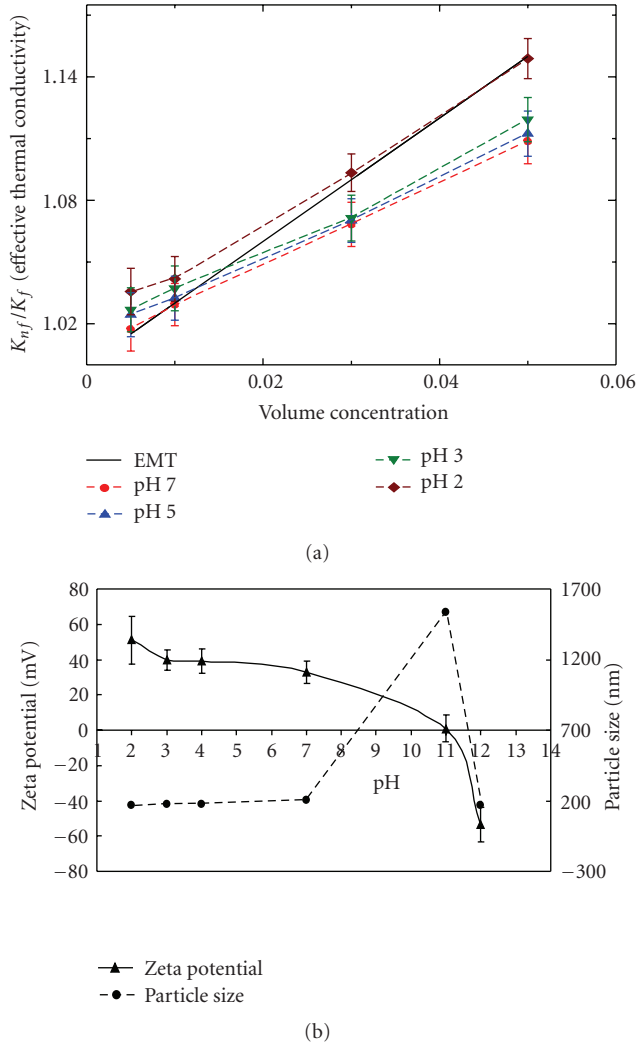

Figure 7: Effect of pH value on (a) thermal conductivity of DI water-based alumina nanofluids and (b) particle size.

increased. On the other hand, the size increase of particles reduces the particle motions which have been proposed to entrain the motion of the fluid for promoting more heat transfer. As a result, the enhancement in thermal conductivity will be reduced. The competition between these two heat transfer mechanisms decides the thermal conductivity enhancement.

To prove this hypothesis, the particle sizes in nanofluids were measured by a Zetasizer machine (Malvern Instruments Ltd), which is based on dynamic light scattering (DLS) technique. In DLS, particles are illuminated with a laser. The intensity of the scattered light fluctuates at a rate that is dependent upon the size of the particles as smaller particles are moved further by the solvent molecules and move more rapidly. Analysis of these intensity fluctuations yields the velocity of the Brownian motion and the particles hydrodynamic size is calculated using the Stokes-Einstein relationship. The results indicate that the average size of particles in the fluids is reduced from 207 nm to around

160 nm when the pH value changes from 7 to 2 (Figure 7(b)). It is also worth noting that the average particle size increases up to 1500 nm when the zeta potential of particle is around zero (pH = 11). It is apparent that a large aggregation occurs when the interparticle repulsion force between particles is small or the surface charge of nanoparticles is small. As the nanofluids become more acidic (lower pH value), more charges are accumulated on the particle surface. Less aggregation occurs and the dispersion is improved. As the result, the effective thermal conductivity increases. For instance, at volumetric fraction of 5%, the thermal conductivity ratio (nanofluids to base fluid) increases from 1.06 to 1.14 (within the error limit). The value of 1.14 is consistent with effective medium theory (EMT) prediction. But the EMT theory fails in taking into consideration the effect of nanoparticle size increase (due to aggregates/clusters formation) on thermal conductivity.

3.3. Effect of Base Fluids on Thermal Conductivity. To study the effect of base fluid property on thermal conductivity in nanofluids, DI water and EG-based alumina nanofluids were measured after they were dispersed using probe type sonicator. Figure 8 shows the trend of thermal conductivity of alumina nanoparticles in different base fluids at different volume concentrations. Apparently, the effective thermal conductivity (ratio of thermal conductivity of nanofluids to that of base fluid) of EG-based alumina nanofluids is higher than that of the DI water-based alumina nanofluids at same concentrations. Unlike DI water-based nanofluids, the thermal conductivity of EG-based alumina nanofluids accurately follows the trend predicted by EMT. One possibility is that in a colloidal system (nanofluids) consisting of a large number of small particles, particles will collide with each other in the course of their Brownian motion. In such a collision, the particles may be so attracted to one another that they stick together to form aggregates. The aggregation rate depends on both the viscosity of base fluid and surface charge of the nanoparticles [43]. A further study on the effect of base fluids on nanofluids thermal conductivity is underway.

3.4. Effect of Nanoparticle Species on Thermal Conductivity. To evaluate the effect of nanoparticle species on thermal conductivity, alumina, copper oxide, and a 1 : 1 mixture of alumina and copper oxide nanoparticles are dispersed in ethylene glycol. The thermal conductivities were measured and presented in Figure 9. The thermal conductivities of alumina (polycrystalline) and copper oxide are reported to be 18 W/m K and 20 W/m K, respectively [36]. The results clearly show that the thermal conductivity of copper oxide nanofluids is higher than that of alumina, which has lower thermal conductivity. But this seems to be not enough to explain the significant difference of thermal conductivities of two nanofluids. In addition, the thermal conductivity of 1 : 1 mixture of alumina and copper Oxide in EG lies in between these two nanofluids (alumina nanofluids and copper oxide nanofluids) at higher concentrations. We hypothesize that a lower interfacial thermal resistance of copper oxide-EG results in a higher thermal conductivity enhancement compared to alumina-EG fluids. This proposed explanation needs a direct measurement of interfacial thermal resistance at the liquid-solid interface, which cannot be conducted in our lab at the current time. The EMT theory, which only takes into account volumetric fraction effect, actually fails in predicting the effects of particle thermal conductivity and interfacial thermal resistance on thermal conductivity.

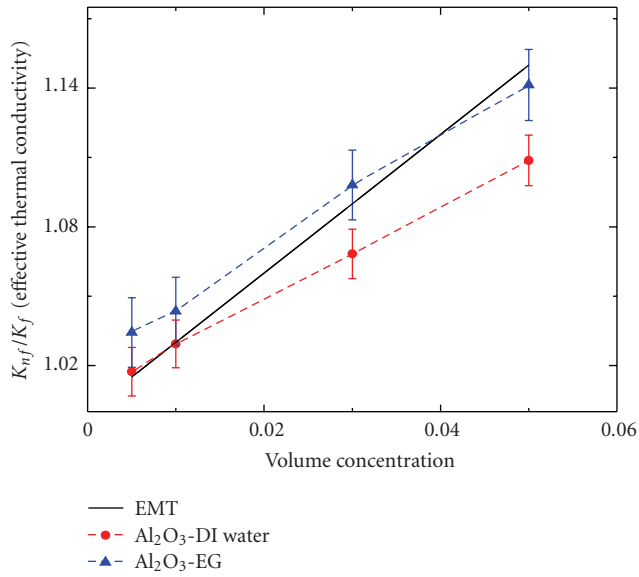

Figure 8: Effect of base fluids (DI water and EG) on thermal conductivity of alumina nanofluids.

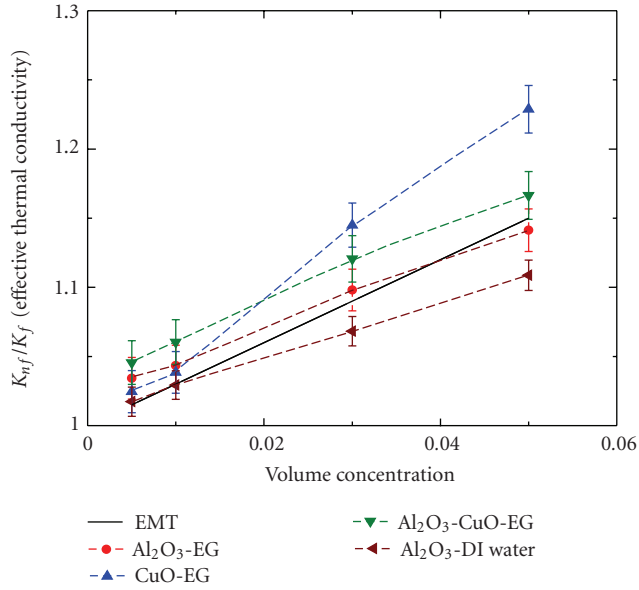

Figure 9: Effect of particle species on thermal conductivities of EG-based alumina, copper oxide, and 1 : 1 mixture of alumina and copper oxide nanofluids.

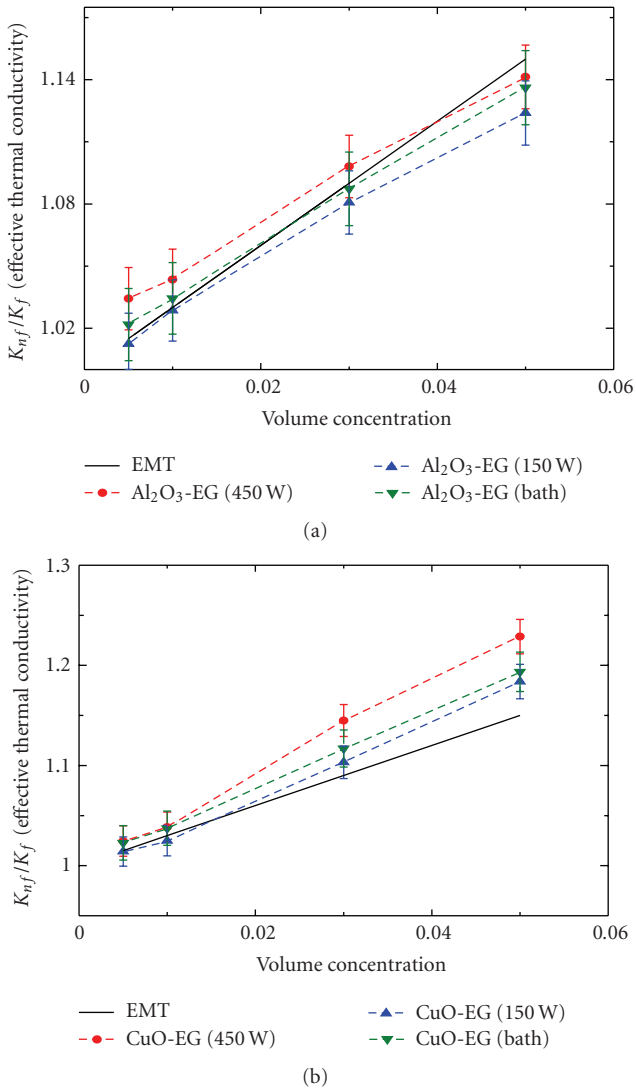

FIGURE 10: Effect of sonication power on thermal conductivities of EG-based (a) alumina and (b) copper oxide nanofluids.

3.5. Effect of Sonication Methods on Thermal Conductivity. Another important parameter to determine thermal conductivity of nanofluids is preparation method. Three sonication methods are used to study the effect of sonication techniques on effective thermal conductivity of nanofluids. All nanoparticles (alumina and copper oxide) are dispersed in EG. The three sonication techniques include: (1) sonication of nanofluids with a probe sonicator (Branson Digital Sonifier 450) at 80% magnitude (maximum power: 450 W) for 2 minutes; (2) another probe sonicator (Omni-Ruptor 250) at 80% magnitude (maximum power: 150 W) for 2 minutes, and (3) a bath sonicator (Model: 75D VWR) for 4.5 hours at maximum power setting (maxium power: 90 W). The measured thermal conductivities are plotted in Figure 10. For both alumina and copper oxide nanofluids, the 450 W probe sonication gave the highest effective thermal conductivity enhancement, followed by bath sonication, and lastly, 150 W probe sonication. Even at lower concentrations (<2%) the trend is still the same but EG-based alumina nanofluids have better effective thermal conductivities compared to EG-based copper oxide nanofluids. The sizes of particles in fluids versus the sonication methods are presented in Figure 11. As we expected, the 450 W probe sonication produces the smallest size (140 nm) of (agglomerated) particles in both DI water and EG-based nanofluids, and the 150 W probe yields larger particle size. Another important observation is that the particle size reduces from 175 nm to 140 nm for EG-based nanofluids compared to a reduction from 155 nm to 140 nm for DI water-based nanofluids. Therefore, sonication technique is more effective for EG-based nanofluids than DI water-based nanofluids. The effective thermal conductivity of nanofluids is directly linked to ultra-sonication power which influences the particle dispersion and average size in the nanofluids. An accurate theory which can incorporate sonication/dispersion criteria is needed to predict thermal conductivities of nanofluids.

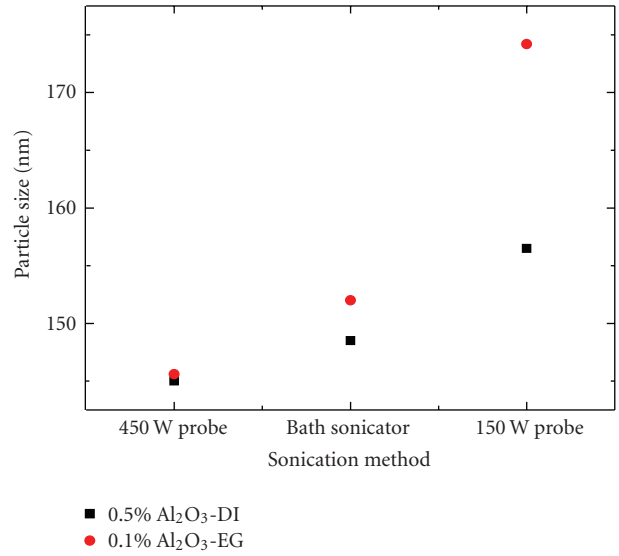

FIGURE 11: Effect of sonication power on (agglomerated) alumina particle size of DI water and EG-based nanofluids.

4. Conclusions

The effect of surface charge (pH value), base fluid, particle species, and dispersion method on thermal conductivity of alumina and copper oxide nanofluids are addressed in a systematic way. The high surface charge (low pH value) of nanofluids improves dispersion of nanoparticles in base fluids. The viscosity of base fluid reduces the Brownian velocity of nanoparticles so that the sedimentation/agglomeration of particles in nanofluids is decreased. All these lead to a higher thermal conductivity. Therefore, the thermal conductivity of nanofluids can be effectively improved by changing pH of fluids and by using more viscous fluids. Another important parameter is dispersion technique. The results demonstrate that high power sonication can significantly improve thermal conductivity of nanofluids and also stability of nanofluids.

Appendix

Uncertainty analysis is given as follows:

$$k = \frac{q}{4\pi L}\left(\frac{Ln(t)}{\Delta T}\right),$$
$$k = f(q, L, t, \Delta T). \tag{A.1}$$

Best estimate for the uncertainty [37] is given as follows:

$$\Delta k = \left[\left(\frac{\partial k}{\partial q}\Delta q\right)^2 + \left(\frac{\partial k}{\partial L}\Delta L\right)^2 + \left(\frac{\partial k}{\partial t}\Delta t\right)^2 + \left(\frac{\partial k}{\partial(\Delta T)}\Delta(\Delta T)\right)^2\right]^{1/2}. \tag{A.2}$$

(1) For $((\partial k/\partial q)\Delta q)$,we have

$$\frac{\partial k}{\partial q} = \frac{1}{4\pi L}\left(\frac{Ln(t)}{\Delta T}\right),$$

$$\Delta q = \left[\left(\frac{\partial q}{\partial V_{\text{in}}}\Delta V_{\text{in}}\right)^2 + \left(\frac{\partial q}{\partial R_w}R_{werr}\right)^2 + \left(\frac{\partial q}{\partial(\Delta R_w)}\Delta(\Delta R_w)\right)^2\right]^{1/2},$$

$$q = \frac{V_{\text{in}}^2(R_w + \Delta R_w)}{(2R_w + \Delta R_w)^2},$$

$$\frac{\partial q}{\partial V_{\text{in}}} = \frac{2V_{\text{in}}(R_w + \Delta R_w)}{(2R_w + \Delta R_w)^2},$$

$$\frac{\partial q}{\partial R_w} = \frac{V_{\text{in}}^2}{(2R_w + \Delta R_w)^2} - \frac{4V_{\text{in}}^2(R_w + \Delta R_w)}{(2R_w + \Delta R_w)^3},$$

$$\frac{\partial q}{\partial(\Delta R_w)} = \frac{V_{\text{in}}^2}{(2R_w + \Delta R_w)^2} - \frac{2V_{\text{in}}^2(R_w + \Delta R_w)}{(2R_w + \Delta R_w)^3},$$

$$\Delta R_w = \frac{4R_w\Delta V}{V_{\text{in}} - 2\Delta V},$$

$$\Delta(\Delta R_w) = \left[\left(\frac{\partial(\Delta R_w)}{\partial R_w}R_{werr}\right)^2 + \left(\frac{\partial(\Delta R_w)}{\partial(\Delta V)}\Delta(\Delta V)\right)^2 + \left(\frac{\partial(\Delta R_w)}{\partial V_{\text{in}}}\Delta V_{\text{in}}\right)^2\right]^{1/2},$$

$$\frac{\partial(\Delta R_w)}{\partial R_w} = \frac{4\Delta V}{V_{\text{in}} - 2\Delta V},$$

$R_{werr} = \pm 0.001\,\Omega$ (DMM multimeter),

$$\frac{\partial(\Delta R_w)}{\partial(\Delta V)} = \frac{4R_w}{(V_{\text{in}} - 2\Delta V)}\left[1 + \frac{2\Delta V}{(V_{\text{in}} - 2\Delta V)}\right],$$

$\Delta(\Delta V) = \pm 0.0018\,\text{V}$ (National Instruments SCXI-1303),

$$\frac{\partial(\Delta R_w)}{\partial V_{\text{in}}} = -\frac{4R_w\Delta V}{(V_{\text{in}} - 2\Delta V)^2},$$

$\Delta V_{\text{in}} = \pm 0.01\%$ Re ading

$+ 3\,\text{mV}$, (National Instruments SCXI-1303),

$\Delta V_{\text{in}} = \pm 0.0038V.$ (A.3)

(2) For $((\partial k/\partial L)\Delta L)$,we have

$$\frac{\partial k}{\partial L} = -\frac{q}{4\pi L^2}\left(\frac{Ln(t)}{\Delta T}\right),$$

$\Delta L = \pm 0.001\,\text{m}$ (ruler or scale). (A.4)

(3) For $((\partial k/\partial t)\Delta t)$,we have

$$\frac{\partial k}{\partial t} = \frac{q}{4\pi L}\left(\frac{1}{\Delta T}\right),$$

$\Delta t = \pm 0.001\,\text{sec}$ (National Instruments SCXI-1303). (A.5)

(4) For $((\partial k/\partial(\Delta T))\Delta(\Delta T))$,we have

$$\frac{\partial k}{\partial(\Delta T)} = -\frac{q}{4\pi L}\left(\frac{Ln(t)}{\Delta T^2}\right),$$

$$\Delta(\Delta T) = \left[\left(\frac{\partial(\Delta T)}{\partial R_w}R_{werr}\right)^2 + \left(\frac{\partial(\Delta T)}{\partial(\alpha)}\Delta\alpha\right)^2 + \left(\frac{\partial(\Delta T)}{\partial(\Delta R_w)}\Delta(\Delta R_w)\right)^2\right]^{1/2},$$

$$\Delta T = \frac{\Delta R_w}{\alpha R_w},$$

$$\frac{\partial(\Delta T)}{\partial(\Delta R_w)} = \frac{1}{\alpha R_w},$$

$$\frac{\partial(\Delta T)}{\partial(\alpha)} = -\frac{\Delta R_w}{\alpha^2 R_w},$$

$$\frac{\partial(\Delta T)}{\partial R_w} = -\frac{\Delta R_w}{\alpha R_w^2},$$

$$\alpha = \frac{dR}{dT},$$

$$\Delta(\alpha) = \left[\left(\frac{\partial\alpha}{\partial(dR)}\Delta(dR)\right)^2 + \left(\frac{\partial\alpha}{\partial(dT)}\Delta(dT)\right)^2\right]^{1/2},$$

$$\frac{\partial\alpha}{\partial(dR)} = \frac{1}{dT},$$

$$\Delta(dR) = R_{werr} = \pm 0.001\,\Omega \text{ (DMM multimeter)},$$

$$\frac{\partial\alpha}{\partial(dT)} = -\frac{dR}{(dT)^2},$$

$$\Delta(dT) = \pm 0.2^{\circ}\text{C (Thermometer)}. \tag{A.6}$$

Nomenclature

K_B: The Boltzmann constant
k_{nf}: Thermal conductivity of the nanoparticle suspension (nanofluids)
k_f: Thermal conductivity of the base fluid
L: Length of the platinum wire
q: Heat generated in the platinum wire
R_w: Resistance of platinum wire at room temperature
t: Time
T: Temperature
V_{in}: Voltage applied to the Wheatstone bridge of the transient hot wire apparatus
α: Temperature coefficient of resistance of the platinum wire
ϕ: Volume fraction of the nanoparticle suspension (nanofluids)
μ: The base fluid dynamic viscosity.

Acknowledgment

The authors would like to acknowledge the support of Nanomanufacturing Center of Excellence (NCOE) Strategic Seed Grant from the State of Massachusetts.

References

[1] J. A. Eastman, S. R. Phillpot, S. U. S. Choi, and P. Keblinski, "Thermal transport in nanofluids," *Annual Review of Materials Research*, vol. 34, pp. 219–246, 2004.

[2] S. Krishnamurthy, P. Bhattacharya, P. E. Phelan, and R. S. Prasher, "Enhanced mass transport in nanofluids," *Nano Letters*, vol. 6, no. 3, pp. 419–423, 2006.

[3] C. H. Chon and K. D. Kihm, "Thermal conductivity enhancement of nanofluids by Brownian motion," *Journal of Heat Transfer*, vol. 127, no. 8, p. 810, 2005.

[4] P. Bhattacharya, S. K. Saha, A. Yadav, P. E. Phelan, and R. S. Prasher, "Brownian dynamics simulation to determine the effective thermal conductivity of nanofluids," *Journal of Applied Physics*, vol. 95, no. 11, pp. 6492–6494, 2004.

[5] R. Prasher, P. Bhattacharya, and P. E. Phelan, "Thermal conductivity of nanoscale colloidal solutions (nanofluids)," *Physical Review Letters*, vol. 94, no. 2, Article ID 025901, 4 pages, 2005.

[6] S. P. Jang and S. U. S. Choi, "Role of Brownian motion in the enhanced thermal conductivity of nanofluids," *Applied Physics Letters*, vol. 84, no. 21, pp. 4316–4318, 2004.

[7] J. Koo and C. Kleinstreuer, "A new thermal conductivity model for nanofluids," *Journal of Nanoparticle Research*, vol. 6, no. 6, pp. 577–588, 2004.

[8] R. Prasher, P. Bhattacharya, and P. E. Phelan, "Brownian-motion-based convective-conductive model for the effective thermal conductivity of nanofluids," *Journal of Heat Transfer*, vol. 128, no. 6, pp. 588–595, 2006.

[9] K.-F. V. Wong and T. Kurma, "Transport properties of alumina nanofluids," *Nanotechnology*, vol. 19, no. 34, Article ID 345702, 8 pages, 2008.

[10] B.-X. Wang, L.-P. Zhou, and X.-F. Peng, "A fractal model for predicting the effective thermal conductivity of liquid with suspension of nanoparticles," *International Journal of Heat and Mass Transfer*, vol. 46, no. 14, pp. 2665–2672, 2003.

[11] K. S. Hong, T.-K. Hong, and H.-S. Yang, "Thermal conductivity of Fe nanofluids depending on the cluster size of nanoparticles," *Applied Physics Letters*, vol. 88, no. 3, Article ID 031901, 3 pages, 2006.

[12] W. Yu and S. Choi, "The role of interfacial layers in the enhanced thermal conductivity of nanofluids: a renovated Hamilton-Crosser model," *Journal of Nanoparticle Research*, vol. 6, no. 4, pp. 355–361, 2004.

[13] Y. Xuan, Q. Li, and W. Hu, "Aggregation structure and thermal conductivity of nanofluids," *AIChE Journal*, vol. 49, no. 4, pp. 1038–1043, 2003.

[14] D. Lee, J.-W. Kim, and B. G. Kim, "A new parameter to control heat transport in nanofluids: surface charge state of the particle in suspension," *Journal of Physical Chemistry B*, vol. 110, no. 9, pp. 4323–4328, 2006.

[15] R. Prasher, P. E. Phelan, and P. Bhattacharya, "Effect of aggregation kinetics on the thermal conductivity of nanoscale colloidal solutions (nanofluid)," *Nano Letters*, vol. 6, no. 7, pp. 1529–1534, 2006.

[16] S. Choi, Z. G. Zhang, W. Yu, F. E. Lockwood, and E. A. Grulke, "Anomalous thermal conductivity enhancement in nanotube suspensions," *Applied Physics Letters*, vol. 79, no. 14, pp. 2252–2254, 2001.

[17] R. Prasher, P. Bhattacharya, and P. E. Phelan, "Brownian-motion-based convective-conductive model for the effective thermal conductivity of nanofluids," *Journal of Heat Transfer*, vol. 128, no. 6, pp. 588–595, 2006.

[18] S. Das, S. Choi, W. Liu, and T. Pradeep, *Nanofluids: Science and Technology*, John Wiley & Sons, New York, NY, USA, 2007.

[19] H. Xie, J. Wang, T. Xi, Y. Liu, and F. Ai, "Dependence of the thermal conductivity on nanoparticle-fluid mixture on the base fluid," *Journal of Materials Science Letters*, vol. 21, no. 19, pp. 1469–1471, 2002.

[20] H. Xie, J. Wang, T. Xi, Y. Liu, F. Ai, and Q. Wu, "Thermal conductivity enhancement of suspensions containing nanosized alumina particles," *Journal of Applied Physics*, vol. 91, no. 7, p. 4568, 2002.

[21] J. A. Eastman, S. Choi, S. Li, W. Yu, and L. J. Thompson, "Anomalously increased effective thermal conductivities of ethylene glycol-based nanofluids containing copper nanoparticles," *Applied Physics Letters*, vol. 78, no. 6, pp. 718–720, 2001.

[22] R. L. Hamilton and O. K. Crosser, "Thermal conductivity of heterogeneous two-component systems," *Industrial and Engineering Chemistry Fundamentals*, vol. 1, no. 3, pp. 187–191, 1962.

[23] S. K. Das, N. Putra, P. Thiesen, and W. Roetzel, "Temperature dependence of thermal conductivity enhancement for nanofluids," *Journal of Heat Transfer*, vol. 125, no. 4, pp. 567–574, 2003.

[24] C. H. Chon, K. D. Kihm, S. P. Lee, and S. Choi, "Empirical correlation finding the role of temperature and particle size for nanofluid (Al_2O_3) thermal conductivity enhancement," *Applied Physics Letters*, vol. 87, no. 15, Article ID 153107, 3 pages, 2005.

[25] M. Chopkar, P. K. Das, and I. Manna, "Synthesis and characterization of nanofluid for advanced heat transfer applications," *Scripta Materialia*, vol. 55, no. 6, pp. 549–552, 2006.

[26] W. Evans, J. Fish, and P. Keblinski, "Role of Brownian motion hydrodynamics on nanofluid thermal conductivity," *Applied Physics Letters*, vol. 88, no. 9, Article ID 093116, 2006.

[27] M. Vladkov and J.-L. Barrat, "Modeling transient absorption and thermal conductivity in a simple nanofluid," *Nano Letters*, vol. 6, no. 6, pp. 1224–1229, 2006.

[28] P. Keblinski and J. Thomin, "Hydrodynamic field around a Brownian particle," *Physical Review E*, vol. 73, no. 1, Article ID 010502, 4 pages, 2006.

[29] W. C. Williams, I. C. Bang, E. Forrest, L. W. Hu, and J. Buongiorno, "Preparation and characterization of various nanofluids," in *Proceedings of the NSTI Nanotechnology Conference and Trade Show (Nanotech '06)*, vol. 2, pp. 408–411, Boston, Mass, USA, May 2006.

[30] V. Trisaksri and S. Wongwises, "Critical review of heat transfer characteristics of nanofluids," *Renewable and Sustainable Energy Reviews*, vol. 11, no. 3, pp. 512–523, 2007.

[31] K. Kwak and C. Kim, "Viscosity and thermal conductivity of copper oxide nanofluid dispersed in ethylene glycol," *Korea-Australia Rheology Journal*, vol. 17, no. 2, pp. 35–40, 2005.

[32] C. Y. Ho, J. Kestin, and W. A. WakeHam, *Transport Properties of Fluids: Thermal Conductivity, Viscosity, and Diffusion Coefficient*, Cindas Data Series on Material Properties, vol. I-1, Hemisphere, New York, NY, USA, 1988.

[33] M. P. Beck, T. Sun, and A. S. Teja, "The thermal conductivity of alumina nanoparticles dispersed in ethylene glycol," *Fluid Phase Equilibria*, vol. 260, no. 2, pp. 275–278, 2007.

[34] S. H. Kim, S. R. Choi, and D. Kim, "Thermal conductivity of metal-oxide nanofluids," *Journal of Heat Transfer*, vol. 129, no. 3, pp. 298–307, 2007.

[35] C. S. Jwo, T. P. Teng, C. J. Hung, and Y. T. Guo, "Research and development of measurement device for thermal conductivity of nanofluids," *Journal of Physics: Conference Series*, vol. 13, pp. 55–58, 2005.

[36] J. Holman, *Heat Transfer*, McGraw-Hill, New York, NY, USA, 9th edition, 2002.

[37] A. Wheeler and A. Ganji, *Introduction to Engineering Experimentation*, Prentice Hall, Upper Saddle River, NJ, USA, 1996.

[38] S. Lee, S. Choi, S. Li, and J. A. Eastman, "Measuring thermal conductivity of fluids containing oxide nanoparticles," *Journal of Heat Transfer*, vol. 121, no. 2, pp. 280–288, 1999.

[39] D. Yoo, K. S. Hong, and H.-S. Yang, "Study of thermal conductivity of nanofluids for the application of heat transfer fluids," *Thermochimica Acta*, vol. 455, no. 1-2, pp. 66–69, 2007.

[40] J. Ma, *Thermal conductivity of fluids containing nanometer sized particles*, M.S. thesis, Department of Mechanical Engineering, MIT, 2006.

[41] X. Wang, X. Xu, and S. Choi, "Thermal conductivity of nanoparticle-fluid mixture," *Journal of Thermophysics and Heat Transfer*, vol. 13, no. 4, pp. 474–480, 1999.

[42] E. V. Timofeeva, A. N. Gavrilov, J. M. McCloskey, et al., "Thermal conductivity and particle agglomeration in alumina nanofluids: experiment and theory," *Physical Review E*, vol. 76, no. 6, Article ID 061203, 2007.

[43] M. von Smoluchowski, "Versuch einer mathematischen theorie der koagulationskinetic kolloider losunger," *Zeitschrift für Physikalische Chemie*, vol. 92, p. 129, 1917.